3 Biotech (2023) 13:343
https://doi.org/10.1007/s13205-023-03717-6

ORIGINAL ARTICLE

Purification and characterization of extracellular lipase from a thermotolerant strain: *Bacillus subtilis* TTP-06

Manpreet Kaur[1] · Rakesh Kumar[2] · Poonam Katoch[3] · Reena Gupta[1]

Received: 1 April 2023 / Accepted: 27 July 2023 / Published online: 12 September 2023

Abstract

In current study, lipase from a thermotolerant *Bacillus subtilis* TTP-06 was purified in a stepwise manner by using ammonium sulfate precipitation and column chromatography. Thenceforth, it was subjected to sodium dodecyl sulfate- and native-polyacrylamide gel electrophoresis to check the homogeneity of the purified enzyme. The ideal substrate concentration, pH, temperature, reaction duration and lipase specificity were identified. With a yield of 11.02%, purified lipase displayed activity of 8.51 U/mg. Thenceforward, the homogeneously purified enzyme was considered to be a homo-dimer of 30 kDa subunits. Enzyme had K_m and V_{max} value of 9.498 mM and 19.92 mol mg^{-1} min^{-1}, respectively. Additionally, the matrix-assisted laser desorption ionization-time of flight mass spectrometry (MALDI-TOF MS) method was used to investigate the purified lipase and estimate its 3-D structure, which revealed a catalytic triad of serine, aspartate and histidine.

Keywords *Bacillus subtilis* TTP-06 · Purification · Characterization · SDS-PAGE · Native-PAGE · MALDI-TOF MS

Introduction

Ubiquitous lipases from the hydrolase fold superfamily feature a lattice of H-bonding at their active site that contains a triad of Ser, Asp (Glu) and His (Wang et al. 2018; Melani et al. 2020). These enzymes exhibit features including chemo-, regio- and stereo-specificity as well as the capacity to perform heterogeneous reactions. They are substrate-specific enzymes. Lipases are widely utilized as biocatalysts in a variety of sectors, including the production of surfactants, detergents, agrochemicals, pharmaceuticals and tanning products (Ananthi et al. 2014; Chandra et al. 2020; Barik et al. 2022). Higher temperature reactions improve the rate of diffusion, make lipids and other hydrophobic substrates more soluble in water and lower the likelihood of contamination (Hamdan et al. 2021). The tolerance of lipases to solvents, high acidic and alkaline environments and substrate specificity are all broader (Febriani et al. 2020). Bacteria are the most notable suppliers of thermostable lipases. Significantly, the *Bacillus* sp. produces lipases that are important for commercial applications (Haniya et al. 2023). Using ammonium sulfate precipitation and ion-exchange chromatography, 55 kDa lipase from *Bacillus safensis* was recently isolated in a stepwise method which exhibited lipase activity and yield of 13.71 U/mg and 16.16%, respectively (Patel and Parikh 2022). In a different study, *Geobacillus stearothermophilus* GS (LGS) lipase had the highest activity at pH 7.5 and stability up to 70°C after 12 h, while lipase from *Anoxybacillus flavithermuscell* showed stability up to 90°C after 12 h and at pH 8.0. (Najm and Walsh 2022).

Lipases are co-factor-independent and continue to function in organic solvents (Chandra et al. 2020). Some of the characteristics that make lipases more suitable biocatalysts include consumption of all different types of glycerides and free fatty acids (FAs) in a transesterification process, high production in non-aqueous medium, quick reaction times and resilience to low pH (Alabdalall et al. 2021). Lipases can be derived from plants, animals or microorganisms, but microbial lipases are the most frequently used class of enzymes in biotechnological applications because they have higher catalytic activity, are independent producers, are easy to genetically modify for desired characteristics, are produced in large quantities and use

✉ Reena Gupta
reenagupta_2001@yahoo.com

[1] Department of Biotechnology, Himachal Pradesh University, SummerHill, Shimla, HP, India

[2] Microbial Type Culture Collection and Gene Bank (MTCC), CSIR-Institute of Microbial Technology, Chandigarh, India

[3] Jaypee University of Information Technology, Waknaghat, Solan, India

less expensive growth culture media (Mehta et al. 2018; Zhao et al. 2021).

Microbial lipases have been purified, characterized from *Bacillus thermocatenulatus* (Kajiwara et al. 2020), *Geobacillus thermoleovorans* (Moharana et al. 2019), *Pichia pastoris* (Furqan and Akhmaloka 2020), *Thermomicrobium roseum* (Yakun et al. 2021), *Thermomyces dupontii* (Javed et al. 2018; Chandra et al. 2020; Adetunji and Olaniran 2021; Li et al. 2022). Previously, a novel thermostable alkaline lipase isolated from *Bacillus subtilis* EH 37 has been purified which showed 17.8-fold purification (Ahmed et al. 2010). Lipase from an extremophilic *B. subtilis* NS 8 showed high stability with half-life of 273.38 min (approximately 4.5 h) at 60°C (Olusesan et al. 2011). Lipase from B. subtilis LP had K_m and V_{max} values of 18.3 mM and 680 U/mg, respectively (Yasar et al. 2020).

In the present investigation, lipase from thermotolerant *B. subtilis* TTP-06 has been purified and characterized. The purified enzyme showed a better purification fold, better thermal stability and high catalytic efficiency. Further, 3-D structure of the purified lipase has been predicted and it was noted that the current lipase demonstrates aspects that are relevant to industry.

Experimental

Materials and methods

Bacterial culture used for the production of lipase was isolated from a hot spring of Tattapani (31.2487° N, 77.0878° E) situated in Himachal Pradesh, India, at an altitude of 2,182 feet above the sea level. The isolate was identified as *B. subtilis* TTP-06 and its sequence was submitted to NCBI (Accession No.: MW828331.1). Sigma Aldrich (U.S.A.) or HIMEDIA (Mumbai, India) provided all of the analytical grade, high purity chemicals that were employed in the current experiment.

Production conditions

A loopful of inoculum from pure culture of *B. subtilis* TTP-06 was aseptically transferred to 50 ml nutrient medium to prepare seed culture. It was then incubated with continuous shaking (150 rpm) for 24 h at 55°C. 0.75% (v/v) inoculum from seed culture was further transferred to 50 ml production medium (pH 7.5) containing 2.0% (v/v) olive oil, 2.75% (w/v) glucose, 1.65% (w/v) peptone, 0.3% (w/v) NaCl and 0.05% (w/v) $MgSO_4$. The production medium was then incubated for 24 h at 55°C.

Enzyme assay

Lipase activity was determined by measuring the micromoles of *p*-nitrophenol (*p*-NP) released from the substrate *p*-nitrophenyl palmitate (*p*-NPP) per minute under the standard assay conditions (Winkler and Stuckmann 1979).

The protein was estimated by dye-binding method (Bradford 1976) using standard bovine serum albumin (BSA). One unit of specific activity was defined as the activity of enzyme in units per mg of protein content.

Ammonium sulfate precipitation

Bacillus subtilis TTP-06 was aerobically inoculated to the production medium and harvesting of crude enzyme was done by centrifugation (10,000 rpm for 10 min). This was stirred continuously while the required amount of ammonium sulfate salt was added to achieve 0 to 90% saturation. Centrifugation was done to separate the protein precipitates, which were then reconstituted in a minimal amount of buffer (0.15 M Tris–HCl, pH 8.5). Separate analyses of the enzyme and protein content were performed on the supernatant and reconstituted precipitated fractions.

Dialysis

Precipitated fractions transferred to a dialysis membrane were intensively dialyzed against 0.15 M Tris–HCl buffer so as to thoroughly eliminate ammonium sulfate. Lastly, the dialysate was tested for both protein content and lipase activity.

Ion-exchange chromatography (DEAE-Sepharose)

A column (22 × 1.25 cm with flow rate of 0.5 ml/min) packed with DEAE-Sepharose matrix and pre-equilibrated with 0.15 M Tris–HCl buffer (pH 8.5) was loaded with the concentrated dialyzed sample. For the collection of first 10 fractions (each containing 2 ml), Tris-HCl buffer (pH 8.5) was used. Remaining fractions were collected by using gradients of 0.1, 0.3, 0.5 and 0.7 M NaCl in a stepwise manner. Using a LabIndia 3000^+ UV/Vis spectrophotometer, the absorbance of each fraction was measured at 280 nm. The fractions with maximum absorbance at 280 nm were further selected for the lipase activity assay and protein content assay.

Gel filtration chromatography (Sephadex G-100)

The enzyme fractions from DEAE-Sepharose column chromatography that showed maximum activity were combined and transferred to Sephadex G-100 matrix packed in

a column of 22 × 1.25 cm size. 40 fractions of 2 ml each were eluted using 0.15 M Tris–HCl buffer (pH 8.5) at a flow rate of 0.5 ml/min. At 280 nm, the absorbance of fractions was determined. For further experiments, the fractions with maximal lipase activity were combined. A fold purification calculation was done by comparing the activity of purified enzyme to that of the crude enzyme.

Molecular weight confirmation

To estimate the molecular mass and subunit molecular mass of the concentered samples, SDS- and native-PAGE were performed (Laemmli, 1970). The bands were then analyzed on the gel. To confirm the presence of lipase after electrophoresis, zymography was performed by following the methodology of Ghamari et al. (2015).

Characterization of purified lipase from *Bacillus subtilis* TTP-06

Lipase activity was determined with substrate *p*-nitrophenyl palmitate (10 mM prepared in *iso*-propanol) and Tris–HCl (0.1 M, pH 8.0). The reaction was started by incubating the reaction mixture (2.9 ml Tris–HCl, 60 µl substrate and 40 µl enzyme extract) at 50°C for 10 min. The reaction was stopped by chilling at −20°C for 1 min. and the amount of *p*-nitrophenol released was measured at 410 nm (LabIndia UV/VIS Spectrometer Lambda 12) after bringing the tubes to room temperature.

Buffer pH and lipase activity

Different buffers (sodium citrate, pH 4.0–6.5; glycine–NaOH, pH 8.5–10.5; sodium acetate, pH 4.0–6.0; sodium phosphate, pH 5.5–8.5; potassium phosphate, pH 7.0–9.5; Tris–HCl, pH 6.5–10.0) were used individually in the reaction mixture in order to evaluate the influence of buffer (0.15 M) on the lipase activity.

Buffer molarity and lipase activity

To determine the optimal molarity of the buffer for the highest activity of *B. subtilis* TTP-06 lipase, the molarity of Tris–HCl buffer was varied (0.05, 0.075, 0.1, 0.125, 0.15, 0.175 and 0.2 M).

Reaction duration and lipase activity

Under shaking conditions (120 rpm) at 50°C, the reaction mixture containing purified lipase from *B. subtilis* TTP-06 was incubated for varying time of 2.5, 5, 7.5, 10, 12.5, 15, 17.5, 20, 22.5 and 25 min. Thereafter, the lipase activity was measured.

Temperature and lipase activity

The reaction mixture was incubated at 25, 30, 35, 40, 45, 50, 55, 60, 65 and 70°C separately to examine the impact of reaction temperature on lipase activity. Under the aforementioned ideal conditions, lipase activity at each of the chosen temperature was measured.

Lipase activity in the presence of different substrates

The influence of 10 mM each of *p*-nitrophenyl formate (*p*-NPF), *p*-nitrophenyl acetate (*p*-NPA), *p*-nitrophenyl butyrate (*p*-NPB), *p*-nitrophenyl octanoate (*p*-NPO), *p*-nitrophenyl laurate (*p*-NPL), *p*-nitrophenyl palmitate (*p*-NPP), *p*-nitrophenyl benzoate (*p*-NPBenz) and *p*-nitrophenyl caprylate (*p*-NPC) on lipase activity was explored and enzyme activity was evaluated under optimum parameters.

Substrate concentration and lipase activity

The varying concentrations (5, 10, 15, 20, 25, 30, 35, 40 mM) of selected substrate were used to conduct the reaction with lipase from *B. subtilis* TTP-06 under optimized conditions.

K_m and V_{max} of lipase

By evaluating the reaction velocity at different substrate concentrations, ranging from 5 to 40 mM, the K_m and V_{max} values of lipase were obtained. The Lineweaver–Burk plot was used to calculate K_m and V_{max} values by plotting the reciprocal of the reaction velocity ($1/V$) against the reciprocal of the substrate concentration ($1/[S]$).

Lipase activity in the presence of metal ions

By adding various metal ions, including Mg^{2+}, Na^{+}, Pb^{+}, Co^{2+}, Hg^{2+}, Fe^{3+}, Ca^{2+}, Cu^{2+}, K^{+} and Zn^{2+} separately to the reaction mixture (pH 8.5, 0.1 M Tris–HCl) along with purified lipase, it was possible to determine the effect of metal ions (1 mM) on the activity of purified enzyme. Relative lipase activity in each case was calculated with respect to the control (without metal ion).

In silico structure prediction

The purified lipase from *B. subtilis* TTP-06 was subjected to matrix-assisted laser desorption ionization-time of flight mass spectrometry (MALDI-TOF MS) at the CSIR-Institute of Himalayan Bioresource Technology (CSIR-IHBT), Palampur, (India). In order to learn more about the similarity of the sequence, the mass/charge (m/z) values of the purified lipase from *B. subtilis* TTP-06 acquired by

MALDI-TOF–MS were quoted as query in the MASCOT search engine (http://www.matrixscience.com) (Sharma et al. 2018; Kumar et al. 2020a, b). The NCBI Blast (http://ncbi.nlm.nih.gov/BLAST/) was used to find the close homology and a template for the modeling of three-dimensional structure of the target protein. The protein models from the template were generated using ROBETTA (https://robetta.bakerlab.org) server and subsequent structure analysis was carried out using the MALDI-TOF MS results to locate probable functional sites.

Statistic evaluation

The data obtained for three replicates of the parameters under study were used to determine the standard deviation (S.D.).

Results and discussion

Crude enzyme

When lipase was produced by *B. subtilis* TTP-06, it was found that the crude enzyme extract contained 28.1 mg/ml of protein and 8.5 U/ml of enzyme activity. It had a 0.30 U/mg specific activity.

Ammonium sulfate precipitation

Maximal enzyme activity of 10.4 U/ml and protein content of 18.6 mg/ml was obtained at 60–70% ammonium sulfate saturation. When high concentrations of small, highly charged ions such as ammonium sulfate are added, these groups compete with the proteins to bind to the water molecules. This removes the water molecules from the protein and decreases its solubility, resulting in precipitation. The concentration of ammonium sulfate is gradually increased, and at a specific level, the particular protein can be retrieved (Chen et al. 2015). previously, lipase from a thermo-halophilic bacterium showed optimum specific activity in the 40–60% fraction with 5.34 purification fold and 0.95% yield (Febriani et al. 2020). In another study, crude enzyme filtrate from *B. safensis* when subjected to 60% saturation by ammonium sulfate precipitation gave maximum specific activity and fold purification of 13.71 U/mg and 1.48, respectively (Patel and Parikh 2022).

Purification of lipase using DEAE-Sepharose column

Lipase from *B. subtilis* TTP-06 was purified using DEAE-Sepharose column chromatography. Figure 1 illustrates the elution profile of the lipase. After passing the dialyzed sample through DEAE-Sepharose column, the purified fractions 16–25 that displayed the highest specific activity were combined.

Purification of lipase using Sephadex G-100 column chromatography

Purified fractions 14–19 obtained after Sephadex G–100 column chromatography displayed the highest specific activity (Fig. 2). With DEAE-Sepharose chromatography, there was a 10.97-fold purification and following Sephadex G-100 column chromatography there was a 28.36-fold purification (Table 1). In a recent study, a purification fold of 4.2 has been achieved by ion-exchange chromatography of a partially purified lipase from *B. safensis* (Patel and Parikh 2022). In another study, a thermostable lipase from *P. pastoris* GS115 was purified by affinity chromatography with a purification fold of 11.6 (Furqan and Akhmaloka 2020). Another thermostable lipase from *G. thermodentrificans* has been purified by using gel-filtration chromatography

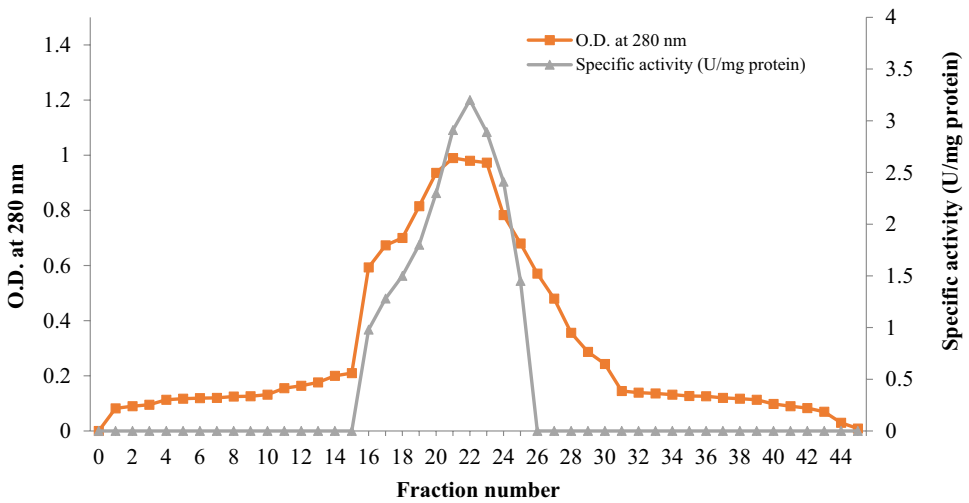

Fig. 1 Elution profile of purified lipase from *Bacillus subtilis* TTP-06 after DEAE-Sepharose column chromatography

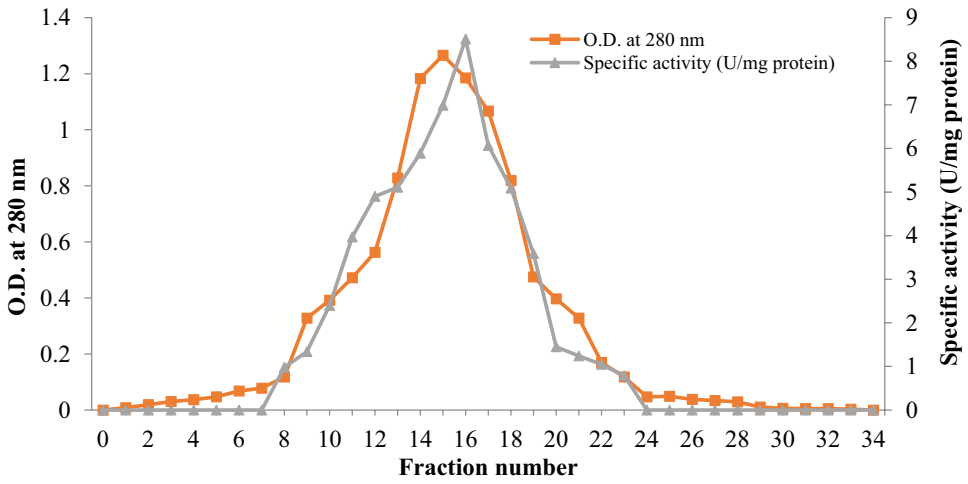

Fig. 2 Elution profile of purified lipase from *Bacillus subtilis* TTP-06 after Sephadex G-100 column chromatography

Table 1 Purification chart of lipase from *Bacillus subtilis* TTP-06

Purification steps	Total lipase activity (U)	Total protein content (mg)	Specific activity (U/mg protein)	Purification fold	Yield (%)
Crude lipase	2550	8430	0.3	1	100
Ammonium sulfate precipitation	2080	3720	0.55	1.83	81.5
DEAE-Sepharose column chromatography	340.5	103.5	3.29	10.97	13.35
Sephadex G-100 column chromatography	281	33	8.51	28.36	11.02

(Sephadex G-100) to achieve a fold-purification and yield of 33.7 and 8.9%, respectively (Balan et al. 2012).

Molecular weight confirmation

Native- and SDS-PAGE gave a single band of 60 kDa and 30 kDa, respectively (Figs. 3, 4). This demonstrated that the enzyme was a dimer and had been homogeneously purified. The purified lipase was confirmed by zymography (Fig. 4).

Previously, a lipase from thermo-halophilic bacterium PLS 80 purified by gel filtration chromatography had a molecular weight of about 50 kDa (Febriani et al. 2020). A recombinant purified lipase from *T. roseum* DSM 5159 had shown a band of approximately 38 kDa on SDS-PAGE (Fang et al. 2021).

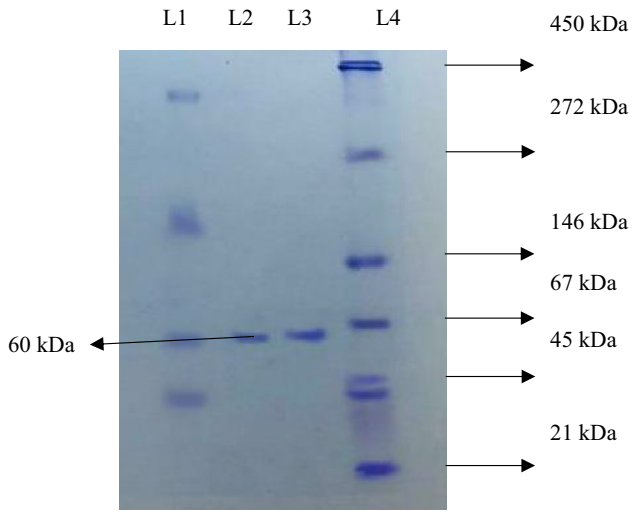

Fig. 3 Native-PAGE of lipase purified from *Bacillus subtilis* TTP-06. L 1: dialyzed fraction, L 2 and L 3: purified lipase enzyme, L 4: SERVA native protein marker (high range molecular weight)

Characterization of purified lipase from *Bacillus subtilis* TTP-06

Buffers pH and lipase activity

Purified lipase from *B. subtilis* TTP-06 gave the highest specific activity (8.93 ± 1.03 U/mg protein) with 0.15 M Tris–HCl buffer at pH 9.0 (Table 2). The enzyme activity dropped as the pH of Tris–HCl buffer was further raised. These findings suggest that the lipase from *B. subtilis* TTP-06 performed well in buffers with an alkaline pH range and poorly in buffers with an acidic pH range. The majority of bacterial lipases have an alkaline pH. It has been found that strains of *Choromobacterium viscosum, Acinetobacter radioresistens* and other species of *Bacillus*, *Micrococcus, Pseudomonas* all produce alkaline

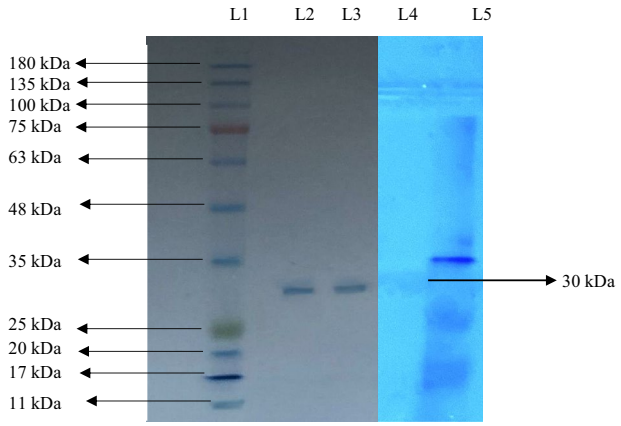

Fig. 4 SDS-PAGE of lipase purified from *Bacillus subtilis* TTP-06. L 1: BR BIOCHEM BLUeye prestained SDS protein marker (medium range molecular weight), L 2,3: purified lipase enzyme. L 4: zymogram of purified lipase, L 5: marker

lipases that function best in the pH range of 9.0–11.0 (Borrelli and Trono 2015; Zhao et al. 2022). A change in pH would have an impact on intramolecular hydrogen bonding, resulting in a distorted conformation and a decrease in the enzyme activity. When the pH was lower, the enzyme was inactivated. Nevertheless, pH extremes result in a temperature- and time-dependent, basically irreversible denaturation (Mehta et al. 2018). A lipase secreted by bacteria found in the intestines of a lepidopteran larva (*Samia ricini*) performed best in the pH range of 7.0 to 9.0 (MsangoSoko et al. 2022).

Buffer molarity and lipase activity

0.1 M Tris–HCl buffer (pH 9.0) yielded the highest specific activity of 9.37 ± 0.15 U/mg protein (Fig. 5). The enzyme activity decreased as the Tris–HCl buffer concentration was raised further. The ionic strength of the solution is a crucial factor that affects the activity of an enzyme. Hence, the ionic composition of the medium affects both the binding of charged substrates to enzymes and the mobility of charged groups inside the catalytic "active" sites. The ionic strength of the solution is strong at higher buffer concentrations and as the buffer concentration is decreased the ionic strength drops and the enzyme effectiveness is reduced (Mehta et al. 2018). In a prior investigation, it was found that the lipase produced by *Bacillus methylotrophicus* PS3 was stable in a 20 mM Tris–HCl buffer with a pH of 8.0 (Sharma et al. 2017).

Reaction duration and lipase activity

Maximum activity (9.86 ± 0.73 U/mg protein) of lipase from *B. subtilis* TTP-06 was observed after 12.5 min of incubation (Fig. 6). A decline in lipase activity was observed as reaction time was extended further. If the enzyme is incubated for a longer duration of time at the enzyme assay temperature, denaturation of the enzyme or product inhibition may lead to a decrease in lipase activity (Xie et al. 2016; Kumar et al. 2020a, b). Lipase produced from a thermo-halophilic bacterium PLS 80 has been known to exhibit maximum enzyme activity after 15 min of incubation (Febriani et al. 2020).

Table 2 Buffer system and lipase activity

pH	Buffer					
	Sodium citrate (0.15 M)	Glycine-NaOH (0.15 M)	Sodium acetate (0.15 M)	Sodium phosphate (0.15 M)	Potassium phosphate (0.15 M)	Tris–HCl (0.15 M)
Specific activity (U/mg protein)						
4.0	3.75 ± 0.3		4.65 ± 0.18			
4.5	3.37 ± 0.2		5.66 ± 0.23			
5.0	5.35 ± 0.5		5.02 ± 0.14			
5.5	4.05 ± 0.5		4.73 ± 0.11	4.64 ± 0.79		
6.0	3.80 ± 0.7		4.35 ± 0.41	4.75 ± 0.95		
6.5	3.03 ± 0.9			4.98 ± 0.58		5.47 ± 0.98
7.0				5.26 ± 0.93	4.55 ± 0.41	5.55 ± 0.93
7.5				5.47 ± 0.50	4.19 ± 0.23	5.78 ± 0.71
8.0				5.64 ± 0.66	5.63 ± 0.64	6.17 ± 0.81
8.5		4.91 ± 0.25		4.46 ± 0.82	5.16 ± 0.21	6.26 ± 0.98
9.0		5.57 ± 0.57			4.88 ± 0.52	**8.93 ± 1.03**
9.5		5.47 ± 0.12			3.63 ± 0.37	5.02 ± 0.93
10.0		5.45 ± 0.32				4.07 ± 0.84
10.5		5.35 ± 0.78				

The enzyme was incubated at 37°C in different buffers (0.15 M) of different pH values for 10 min. Values are mean ± S.D. of three observations

Bold text in Table refers to the maximum activity involved in the particular parameter

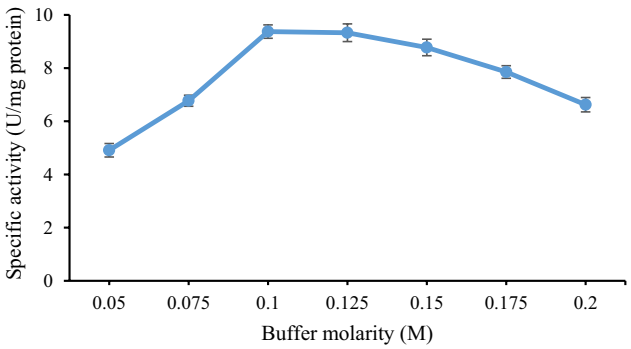

Fig. 5 Effect of buffer molarity on the activity of purified lipase

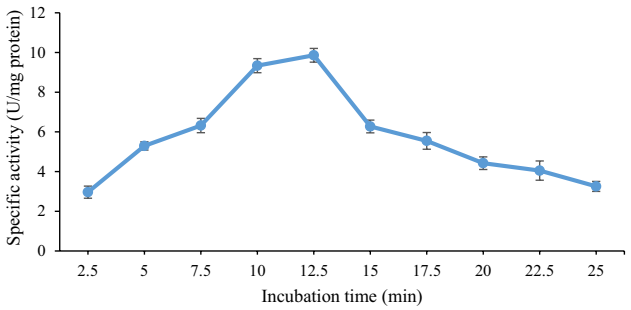

Fig. 6 Effect of reaction time on the activity of purified lipase

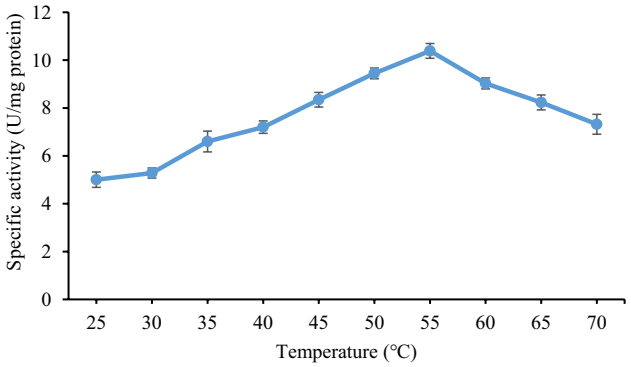

Fig. 7 Effect of reaction temperature on the activity of purified lipase

Reaction temperature and lipase activity

While examining how temperature affects the activity of purified lipase from *B. subtilis* TTP-06, the maximum enzyme activity (10.38 ± 0.82 U/mg protein) was found at 55°C (Fig. 7). When temperature was increased further from 55 to 70°C, a drop in enzyme activity was seen. The structure of an enzyme changes at higher temperatures either as a result of the enzyme denaturation or as a result of the enzyme being more flexible to widen its active site for the best possible substrate binding. An initial increase in activity may have been brought on by the increasing average kinetic energy of the reactants, which in turn increase the likelihood of an effective collision between them. According to a study, *Pseudomonas aeruginosa* HFE733 lipase had the highest activity at 40°C, which was comparable to the corresponding temperature for other lipases from *Burkholderia* sp. ZYB002 and *P. aeruginosa* LX1 (Hu et al. 2018). In another study, ideal temperature for *Acinetobacter* sp. AU07 lipase activity was 50℃ (Gururaj et al. 2016). Lipase from a thermo-halophilic bacterium PLS 80 had shown highest specific activity of 233.4 U/mg at 70°C (Febriani et al. 2020). A thermotolerant recombinant TDL2 lipase from *T. dupontii* was found to be stable at 50°C (Li et al. 2022).

Table 3 Lipase activity in the presence of different substrates

Substrate (10 mM)	Specific activity (U/mg protein)	Relative activity (%)
p-NPP	10.38 ± 1.43	100
p-NPB	5.81 ± 0.67	55.97
p-NPA	5.26 ± 0.82	50.67
p-NPBenz	6.34 ± 0.63	61.07
p-NPF	3.92 ± 0.29	37.76
p-NPO	8.09 ± 0.93	77.93
p-NPL	9.37 ± 1.05	90.26
p-NPC	8.75 ± 0.58	84.29

The enzyme was incubated at 55°C in 0.1 M Tris–HCl buffer (pH 9.0) for 12.5 min with different substrates (10 mM) separately. Values are mean ± S.D. of three observations

Lipase activity in the presence of different substrates

The purified lipase displayed the strongest affinity for *p*-NPP (Table 3). Substrate specificity is affected by complementary shapes, charges and hydrophilic/hydrophobic properties of the substrates and the enzymes. While being able to hydrolyze substrates with various acyl chains in the current investigation, purified lipase exhibited a preference for those with longer chain lengths. A novel thermostable lipase from *Serratia* sp. scl1 exhibited maximum activity with *p*-NPP as substrate (Ali et al. 2022). However, another study indicated that a recombinant lipase TDL2 from *T. dupontii* had the highest specific activity for *p*-nitrophenyl laurate and medium- and long-chain substrates (Li et al. 2022). Another thermostable lipase from *Pseudomonas putida* hydrolyzed *p*-nitrophenyl palmitate effectively to *p*-nitrophenol (Singh and Mehta 2022).

Substrate concentration and lipase activity

Lipase from *B. subtilis* TTP-06 gave maximum activity with substrate (*p*-NPP) concentration of 20 mM (Fig. 8).

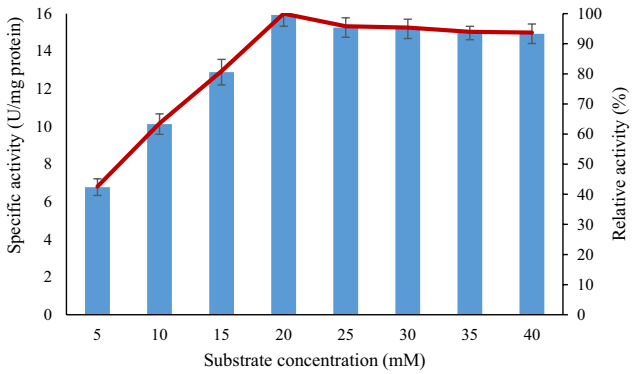

Fig. 8 Effect of substrate concentration on the activity of purified lipase

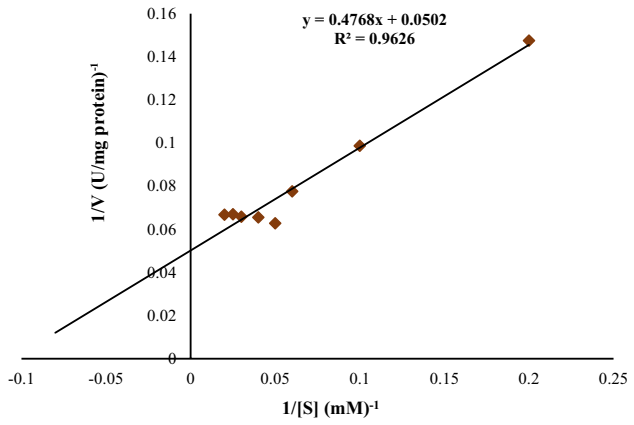

Fig. 9 Lineweaver–Burk plot for lipase from *Bacillus subtilis* TTP-06

Appropriate substrate concentration is necessary for better activity, otherwise low and high concentration beyond optimum leads to decrease in activity due to a decrease in binding efficiency of substrate to active site on enzyme. The active sites of enzyme may not be saturated at low substrate concentrations, and as a result, rising substrate concentrations leads to an increase in enzyme activity (Singh and Mehta 2022). In a recent study, lipase from *Serratia* sp. scl1was found to be saturated when the concentration of *p*-NPP reached 1.3 mM (Ali et al. 2022). Another thermostable lipase from *P. putida* got saturated at 2 mM *p*-NPP concentration (Singh and Mehta 2022).

K_m and V_{max} of lipase

K_m and V_{max} values of the lipase from *B. subtilis* TTP-06 were determined from the linear regression analysis of $1/V$ versus $1/[S]$. Using *p*-NPP as substrate, K_m and V_{max} values were calculated to be 9.498 mM and 19.92 µmol mg^{-1} min^{-1}, respectively (Fig. 9). The K_m of an enzyme in relation to the concentration of its substrate under ideal conditions allows one to estimate whether or not the availability of the substrate will have an impact on the rate of product formation. The main determinant of the affinity of an enzyme for its substrate is K_m, which also has an impact on how quickly the enzyme becomes saturated with its substrate. When the K_m value is low, the affinity of an enzyme for a substrate is high; when K_m value high, the enzyme's affinity is low (Gururaj et al. 2016). In a previous study, K_m and V_{max} values of a lipase from *Aspergillus fumigatus* came out to be 9.89 mM and 10.42 µmol min^{-1} mg^{-1}, respectively (Mehta et al. 2018). A thermostable lipase from *P. putida* had K_m and V_{max} values of 0.62 mM and 355.7 µmol min^{-1} min^{-1} respectively (Singh and Mehta 2022).

Stability of purified enzyme at different temperatures

The purified lipase was stable up to 55°C for about 8 h of incubation. However at 60°C, the half-life of lipase was observed to be 5.5 h (Fig. 10). Purified enzyme retained 67.67% and 24.73% of its original activity at 55°C and 60°C, respectively, after 8 h of incubation. Thermal energy, unlike extremes of pH and low water activity, penetrates across the cell envelope. Therefore, cellular components of thermophiles have adapted to function at high temperatures. It is the activity and stability of cellular components such as proteins, ribosomes, nucleic acids and membranes at high temperatures that forms the basis of thermophilicity of the source organism and thermostability of proteins. In a similar study, thermostable lipase Lk1 from *P. pastoris* GS115 maintained 50% activity after 3 h of incubation (Furqan and Akhmaloka 2020). In a recent study, a thermostable lipase from *Bacillus. thermoruber* strain 7 had a half-life of 5 h at 60°C (Atanasova et al. 2023). Thermostability of lipases can be attributed to certain characteristics including a relatively small hydrophobic surface, exposed N- and C-termini

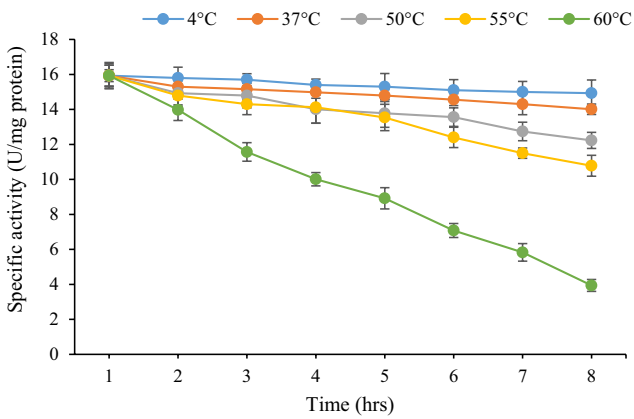

Fig. 10 Thermostability profile of purified lipase

loops, strong ion-pairing with arginine residues, hydrogen and disulfide bonds, interactions between aromatic pairs and hydrophobic interactions (Hamdan et al. 2021).

Lipase activity in the presence of metal ions

The lipase activity of *B. subtilis* TTP-06 was inhibited by each of the metal ions that were investigated. In instance, the lipase activity was less inhibited by the addition of 1 mM Ca^{2+}, Mg^{2+}, K^{+}, Fe^{3+} and Na^{+}. However, Hg^{2+} and Co^{2+} substantially decreased enzyme activity when compared to the control (Table 4). It is most likely because the lipase enzyme does not need a cofactor. Salt ions frequently serve as cofactors and occasionally, as competitive inhibitors. They either increase or decrease the activity of the enzyme. Metalloenzymes contain metals that function as electrophilic catalysts, stabilize any elevated electron density or negative charge that might have arisen during reactions. Stability of such enzymes is improved by metal ions. Ca^{2+} and K^{+} ions boost lipase activity by causing the enzyme to undergo significant conformational rearrangement upon their binding activity (Wang et al. 2012). Additionally, according to a study Ca^{2+} ion therapy increased *B. subtilis* 168 lipase activity (Lesuisse et al. 1993).

Structure determination (in silico) of purified lipase

The results obtained from MALDI-TOF–MS analyzed by Mascot search had the highest score (53), mass (46,556 Da), and protein sequence coverage of 27% with Lipase OS (*Bacillus* sp. OX = 1409) (Fig. 11). A higher MASCOT score means that it contains more peptides from a given protein (Sharma et al. 2018). To forecast the 3-D structure of *B. subtilis* TTP-06 lipase, a template-based modeling (homology modeling or comparative modeling) method was used. The 3-D structure of lipase was predicted by uploading the sequence to ROBETTA (https://robetta.bakerlab.org) server and subsequent structural analysis revealed the presence of three active site residues, namely serine, aspartate and histidine (Fig. 12). It can be assumed that active site residues in purified lipase retained the spatial geometry and polar contacts necessary for optimal lipase activity since the in silico study identified the presence of the catalytic triad. The generated structure was verified by ERRAT score (Fig. 13a) and Ramachandran plot (Fig. 13b). Figure 13a shows an ERRAT score of 95.343% which was quite close to the overall quality factor. The plot (Fig. 13b) showed that the constructed model is of good quality as 88.1% region of Ramachandran plot falls in favored regions. In a similar study, the 3 D structure of the lipase from *Rhizopus oryzae* was built using homology modelling. The predicted 3 D model was validated using the SWISS model validation server. Ramachandran and ERRAT plots were used to assess the amino acid environment and overall quality of the model (Ayinla et al. 2022). In another recent study, 3-dimensional structural model of *Aspergillus flavus* lipase was found to share 34.08% sequence identity with a lipase from *Yarrowia lipolytica* covering 272 amino acid residues of the template model (Ezema et al. 2022).

Table 4 Effect of metal ions on the activity of lipase from *Bacillus subtilis* TTP-06

Metal ion (1 mM)	Specific activity (U/mg protein)	Relative activity (%)
Control	15.93 ± 0.78	100
Mg^{2+}	15.53 ± 0.59	97.5
Na^{+}	15.26 ± 1.03	95.8
Pb^{+}	14.44 ± 0.82	90.7
Co^{2+}	11.82 ± 0.38	74.2
Hg^{2+}	11.31 ± 0.37	71.0
Fe^{3+}	15.32 ± 0.86	96.2
Ca^{2+}	15.59 ± 0.59	97.9
Cu^{2+}	14.60 ± 0.55	91.7
K^{+}	14.87 ± 1.21	93.4
Zn^{2+}	14.83 ± 0.44	93.1

The enzyme was incubated at 55°C in 0.1 M Tris–HCl buffer (pH 9.0) for 12.5 min in presence of different metal ions (1 mM) separately. A control without metal ion was also run. Values are mean ± S.D. of three observations

Conclusion and future perspective(s)

Lipase from thermotolerant *B. subtilis* TTP-06 was purified to homogeneity and was found to be a dimer of 30 kDa by SDS and Native-PAGE analysis. The purified enzyme was stable at 55°C for about 8 h. The amino acid sequence obtained by MALDI-TOF–MS analysis of purified lipase from thermotolerant *B. subtilis* TTP-06 shared similarity with Lipase OS from *Bacillus* sp. 3-D structure of purified lipase was determined by performing template-based modeling (homology or comparative modeling) which revealed the presence of three active site residues (i.e., serine, aspartate and histidine). An ERRAT score of 95.343% verified the generated 3-D structure. Ramachandran plot also verified the model quality. The catalytic triad is important for protein-substrate interactions so a relationship could be postulated in the structure and activity of lipase from *B. subtilis* TTP-06. Further docking studies could be done to study the binding energies of different substrates/molecules with the amino acids present in the active pocket of the enzyme.

MATRIX SCIENCE **MASCOT Search Results**

Protein View: LIP_BACSP

Lipase OS=Bacillus sp. OX=1409 PE=1 SV=3

Database:	SwissProt
Score:	53
Expect:	2.6
Monoisotopic mass (M$_r$):	46556
Calculated pI:	6.50
Taxonomy:	Bacillus sp. (in: Bacteria)

Sequence similarity is available as an NCBI BLAST search of LIP_BACSP against nr.

Search parameters

Enzyme:	Trypsin: cuts C-term side of KR unless next residue is P.
Fixed modifications:	Carboxymethyl (C)
Variable modifications:	Oxidation (M)
Mass values searched:	10
Mass values matched:	6

Protein sequence coverage: 27%

Matched peptides shown in ***bold red***.

```
  1 MKCCRIMFVL LGLWFVFGLS VPGGRTEAAS LRANDAPIVL LHGFTGWGRE
 51 EMFGFKYWGG VRGDIEQWLN DNGYRTYTLA VGPLSSNWDR ACEAYAQLVG
101 GTVDYGAAHA AKHGHARFGR TYPGLLPELK RGGRIHIIAH SQGGQTARML
151 VSLLENGSQE EREYAKAHNV SLSPLFEGGH HFVLSVTTIA TPHDGTTLVN
201 MVDFTDRFFD LQKAVLEAAA VASNVPYTSQ VYDFKLDQWG LRRQPGESFD
251 HYFERLKRSP VWTSTDTARY DLSVSGAEKL NQWVQASPNT YYLSFSTERT
301 YRGALTGNHY PELGMNAFSA VVCAPFLGSY RNPTLGIDDR WLENDGIVNT
351 VSMNGPKRGS SDRIVPYDGT LKKGVWNDMG TYNVDHLEII GVDPNPSFDI
401 RAFYLRLAEQ LASLRP
```

Unformatted sequence string: 416 residues (for pasting into other applications).

Sort by ◉ residue number ○ increasing mass ○ decreasing mass
Show ◉ matched peptides only ○ predicted peptides also

Start – End	Observed	Mr(expt)	Mr(calc)	Delta	M	Peptide
33 – 49	1823.9551	1822.9478	1822.9479	0.0000	0	R.ANDAPIVLLHGFTGWGR.E
135 – 148	1488.8020	1487.7947	1487.7957	-0.0010	0	R.IHIIAHSQGGQTAR.M
163 – 166	510.2558	509.2485	509.2485	0.0000	0	R.EYAK.A
167 – 207	4433.1982	4432.1909	4432.1911	-0.0002	0	K.AHNVSLSPLFEGGHHFVLSVTTIATPHDGTTLVNMVDFTDR.F
214 – 235	2343.1866	2342.1793	2342.1794	-0.0001	0	K.AVLEAAAVASNVPYTSQVYDFK.L
341 – 357	1873.9112	1872.9039	1872.9040	-0.0001	0	R.WLENDGIVNTVSMNGPK.R

No match to: 2166.0284, 3856.3658, 7823.9850, 10000.2356

Fig. 11 MASCOT search results of MALDI-TOF MS spectrum of peptides (tryptic digest) of purified lipase from *Bacillus subtilis* TTP-06

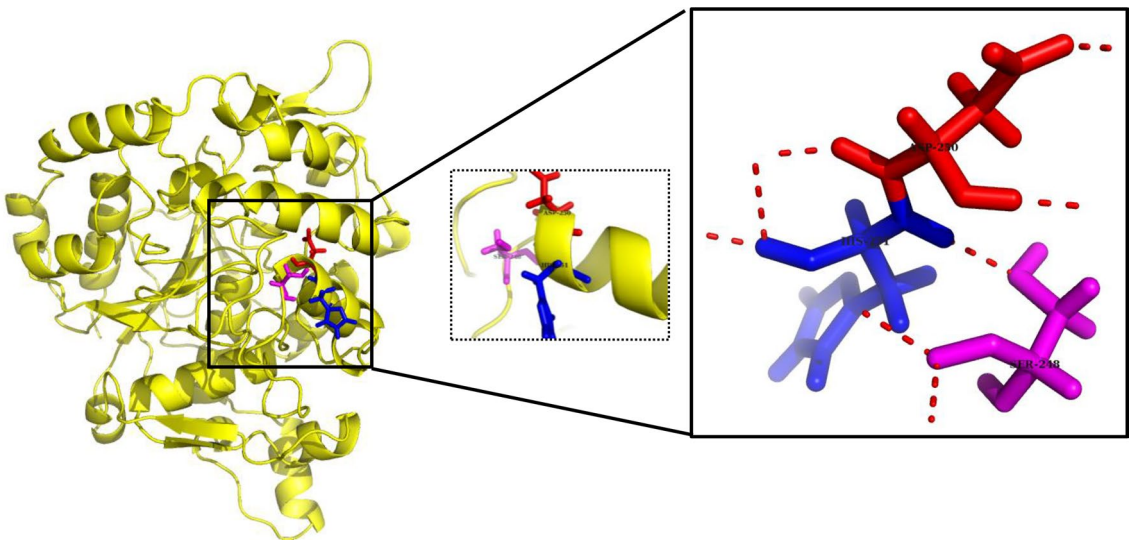

Fig. 12 3-D structure of lipase from *Bacillus subtilis* TTP-06 predicted using ROBETTA server showing active site residues (catalytic triad), i.e., serine (purple), aspartate (red), histidine (blue)

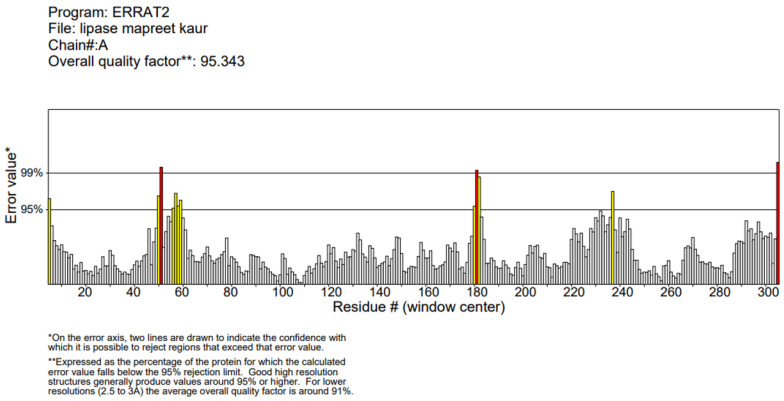

(a)

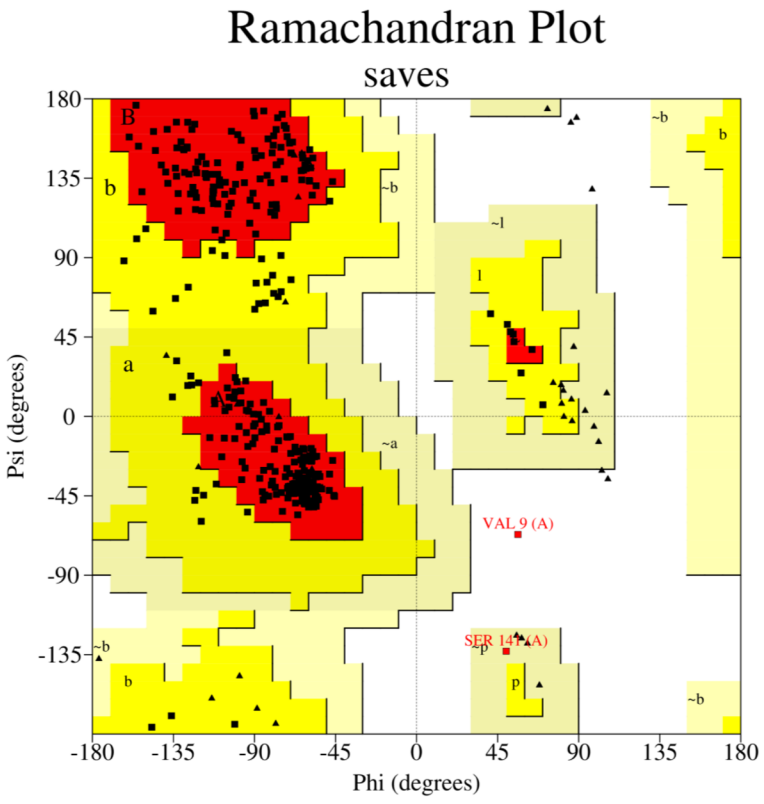

Plot statistics

Residues in most favoured regions [A,B,L]	312	88.1%
Residues in additional allowed regions [a,b,l,p]	40	11.3%
Residues in generously allowed regions [~a,~b,~l,~p]	1	0.3%
Residues in disallowed regions	1	0.3%
Number of non-glycine and non-proline residues	354	100.0%
Number of end-residues (excl. Gly and Pro)	1	
Number of glycine residues (shown as triangles)	42	
Number of proline residues	19	
Total number of residues	416	

Based on an analysis of 118 structures of resolution of at least 2.0 Angstroms and R-factor no greater than 20%, a good quality model would be expected to have over 90% in the most favoured regions.

(b)

Fig. 13 Model assessment by PROCHECK tool (**a**) ERRAT plot and (**b**) Ramachandran plot of lipase purified from thermotolerant *Bacillus subtilis* TTP-06. It describes the quality of the model and shows that 88.1% region of Ramachandran plot falls in favored regions, thereby specifying a good model quality

Acknowledgements Council of Scientific and Industrial Research (CSIR), Pusa, New Delhi, INDIA, is thankfully acknowledged for providing financial assistance in the form of SRF (Award no.: 09/237(170)/2018-EMR-I). Authors are highly thankful to Department of Biotechnology, Ministry of Science and Technology, Govt. of India, for providing financial support and all necessary facilities to Department of Biotechnology, Himachal Pradesh University, Shimla, India.

Declarations

Conflict of interest Author(s) do not have any competing interest(s).

Ethical statement Present study did not involve human participants and/or animals and hence no consent is required for the same.

References

Adetunji AI, Olaniran AO (2021) Production strategies and biotechnological relevance of microbial lipases: a review. Braz J Microbiol 52:1257–1269

Ahmed EH, Raghavendra T, Madamwar DA (2010) Thermostable alkaline lipase from a local isolate *Bacillus subtilis* EH 37: characterization, partial purification, and application in organic synthesis. Appl Biochem Biotechnol 160:2102–2113. https://doi.org/10.1007/s12010-009-8751-4

Alabdalall AH, Al-Anazi NA, Aldakheel LA, Amer FHI, Aldakheel FA, Ababutain IM, Alghamdi AI, Al-Khaldi EM (2021) Application and characterization of crude fungal lipases used to degrade fat and oil wastes. Sci Rep 11: 19670. https://doi.org/10.1038/s41598-021-98927-4

Ali SR, Sultana SS, Rajak S (2022) *Serratia* sp. scl1: isolation of a novel thermostable lipase producing microorganism which holds industrial importance. Antonie Van Leeuwenhoek 115:1335–1348. https://doi.org/10.1007/s10482-022-01776-y

Ananthi S, Ramasubburayan R, Palavesam A, Immanuel G (2014) Optimization and purifcation of lipase through solid state fermentation by *Bacillus cereus* MSU as isolated from the gut of a marine fsh Sardinella Longiceps. Int J Pharm Pharm Sci 6: 291–298

Atanasova N, Paunova-Krasteva T, Kambourova M, Boyadzhieva IA (2023) Thermostable Lipase Isolated from *Brevibacillus thermorube*r Strain 7 Degrades Ɛ-Polycaprolactone. BioTech 12:23. https://doi.org/10.3390/biotech12010023

Ayinla ZA, Ademakinwa AN, Agboola FK (2022) Comparative modelling, molecular docking and immobilization studies on *Rhizopus oryzae* lipase: evaluation of potentials for fatty acid methyl esters synthesis. J Biomol Struct Dyn. https://doi.org/10.1080/07391102.2022.2119279

Balan A, Ibrahim D, Rahim RA, Rashid FAA (2012) Purification and characterization of a thermostable lipase from *Geobacillus thermodenitrificans* IBRL-nra. Enzyme Res. https://doi.org/10.1155/2012/987523

Barik A, Sen SK, Rajhans G, Raut S (2022) Purification and optimization of extracellular lipase from a novel strain *Kocuria flava* Y4. Int J Anal Chem. https://doi.org/10.1155/2022/6403090

Benjamin O, Ezema OKO, Bill RM, Goddard AD, Eze SOO, Fernandez-Castane A (2022) Bioinformatic characterization of a triacylglycerol lipase produced by *Aspergillus flavus* isolated from the decaying seed of *Cucumeropsis mannii*. J Biomol Struct Dyn. https://doi.org/10.1080/07391102.2022.2035821

Bradford MM (1976) A rapid and sensitive method for the quantitation of microgram quantities of protein utilizing the principle of protein-dye binding. Anal Biochem 72:248–254

Borrelli GM, Trono D (2015) Recombinant lipases and phospholipases and their use as biocatalysts for industrial applications. Int J Mol Sci 16:20774–20840

Chandra P, Enespa SR, Arora PK (2020) Microbial lipases and their industrial applications: a comprehensive review. Microb Cell Fact 26:169. https://doi.org/10.1186/s12934-020-01428-8

Chen S, Zheng X, Cao H, Jiang L, Liu F, Sun X (2015) A simple and efficient method for extraction of Taq DNA polymerase. Electron J Biotechnol 18:355–358

Ezema BO, Omeje KO, Bill RM, Goddard AD, Eze SOO, Fernandez-Castane A (2022) Bioinformatic characterization of a triacylglycerol lipase produced by *Aspergillus flavus* isolated from the decaying seed of Cucumeropsis mannii. J Biomol Struct Dyn 41:2587–2601

Fang Y, Zhou Y, Xin Yu, Shi YI, Guo Z, Li Y, Gu Z, Ding Z, Shi G, Zhang L (2021) Preparation and characterization of a novel thermostable lipase from *Thermomicrobium roseum*. Catal Sci Technol 11:7386–7397

Febriani AN, Kemala P, Saidi N, Iqbalsyah TM (2020) Novel thermostable lipase produced by a thermo-halophilic bacterium that catalyses hydrolytic and transesterification reactions. Heliyon 6:2405–8440. https://doi.org/10.1016/j.heliyon.2020.e04520

Furqan BRN, Akhmaloka (2020) Heterologous expression and characterization of thermostable lipase (Lk1) in *Pichia pastoris* GS115. Biocatal Agric Biotechnol 23:1878–8181. https://doi.org/10.1016/j.bcab.2019.101448

Ghamari M, Alemzadeh I, Yazdi FT, Vossoughi M, Varidi M (2015) Purification and zymography of lipase from *Aspergillus niger* PTCC5010. Int J Eng Trans B 28:1117–1123

Gururaj P, Ramalingam S, Devi NG, Gautam P (2016) Process optimization for production and purification of a thermostable, organic solvent tolerant lipase from *Acinetobacter* sp. AU07. Brazilian J Microbiol 47:647–657

Hamdan SH, Maiangwa J, Ali MSM, Normi YM, Sabri S, Leow TC (2021) Thermostable lipases and their dynamics of improved enzymatic properties. Appl Microbiol Biotechnol 105:7069–7094. https://doi.org/10.1007/s00253-021-11520-7

Haniya M, Ullah I, Ali U, Abbas N, Hussain Z, Ali SS, Zhu H (2023) Optimization of low-cost solid-state fermentation media for the production of thermostable lipases using agro-industrial residues as substrate in culture of *Bacillus amyloliquefaciens*. Biocatal Agric Biotechnol 47:1878–8181. https://doi.org/10.1016/j.bcab.2022.102559

Hu J, Cai W, Wang C, Du X, Lin J, Cai J (2018) Purification and characterization of alkaline lipase production by *Pseudomonas aeruginosa* HFE733 and application for biodegradation in food wastewater treatment. Biotechnol Biotechnol Equipment 32:583–590

Javed S, Azeem F, Hussain S, Rasul I, Siddique MH, Riaz M, Afzal M, Kouser A, Nadeem H (2018) Bacterial lipases: a review on purification and characterization. Prog Biophys Mol Biol 132:23–34. https://doi.org/10.1016/j.pbiomolbio.2017.07.014

Kajiwara S, Yamada R, Matsumoto T, Ogino H (2020) N-linked glycosylation of thermostable lipase from *Bacillus thermocatenulatus* to improve organic solvent stability. Enzyme Microb Technol. https://doi.org/10.1016/j.enzmictec.2019.109416

Kumar A, Mukhia S, Kumar N, Acharya V, Kumar S, Kumar R (2020a) A broad temperature active lipase purified from a psychrotrophic bacterium of Sikkim Himalaya with potential application in detergent formulation. Front Bioeng Biotechnol 8:642. https://doi.org/10.3389/fbioe.2020.00642

Kumar R, Katwal S, Sharma B, Sharma A, Kanwar SS (2020b) Purification, characterization and cytotoxic properties of bacterial RNase. Int J Biol Macromol 166:665–676

Lesuisse E, Schanck K, Colson C (1993) Purification and preliminary characterization of the extracellular lipase of *Bacillus*

subtilis 168, an extremely basic pH-tolerant enzyme. Eu J Biochem 216:155–160

Li XJ, Li Q, Zhan XX (2022) Expression and characterization of a thermostable lipase from *Thermomyces dupontii*. Chem Papers 76:2811–2821. https://doi.org/10.1007/s11696-022-02068-5

Mehta A, Grover C, Gupta R (2018) Purification of lipase from *Aspergillus fumigatus* using Octyl Sepharose column chromatography and its characterization. J Basic Microbiol 58:857–866

Melani NB, Tambourgi EB, Silveira E (2020) Lipases: from production to applications. Sep Purif Rev 49:143–158

Moharana TR, Pal B, Rao NM (2019) X-ray structure an characterization of a thermostable lipase from *Geobacillus thermoleovorans*. Biochem Biophys Res Commun 508:145–151. https://doi.org/10.1016/j.bbrc.2018.11.105

MsangoSoko K, Gandotra S, Bhattacharya R, Ramakrishnan B, Sharma K, Subramanian S (2022) Screening and characterization of lipase producing bacteria isolated from the gut of a lepidopteran larvae, *Samia ricini*. J Asia Pac Entomol 25:1226–8615. https://doi.org/10.1016/j.aspen.2021.101856

Najm T, Walsh M (2022) Characterization of lipases from *Geobacillus stearothermophilus* and *Anoxybacillus flavithermus* cell lysates. Food Nutr Sci 13:238–251. https://doi.org/10.4236/fns.2022.133020

Olusesan AT, Azura LK, Forghani B, Bakar FA, Mohamed AKS, Radu S, Manap MYA, Saari B (2011) Purification, characterization and thermal inactivation kinetics of a non-regioselective thermostable lipase from a genotypically identified extremophilic *Bacillus subtilis* NS 8. New Biotechnol 28:738–745. https://doi.org/10.1016/j.nbt.2011.01.002

Patel K, Parikh S (2022) Identification, production, and purification of a novel lipase from *Bacillus safensis*. J Appl Biol Biotechnol 10:73–76. https://doi.org/10.7324/JABB.2022.100410

Sharma A, Meena KR, Kanwar SS (2018) Molecular characterization and bioinformatics studies of a lipase from *Bacillus thermoamylovorans BHK67*. Int J Biol Macromol 107:2131–2140

Sharma P, Sharma N, Pathania S, Handa S (2017) Purification and characterization of lipase by *Bacillus methylotrophicus* PS3 under submerged fermentation and its application in detergent industry. J Genet Eng Biotechnol 15:369–377. https://doi.org/10.1016/j.jgeb.2017.06.007

Singh J, Mehta A (2022) The main Aflatoxin B1 degrading enzyme in *Pseudomonas putida* is thermostable lipase. Heliyon 8:2405–8440. https://doi.org/10.1016/j.heliyon.2022.e10809

Wang Y, Ryu BH, Yoo W, Lee CW, Kim KK, Lee JH, Kim TD (2018) Identification, characterization, immobilization, and mutational analysis of a novel acetylesterase with industrial potential (LaAcE) from *Lactobacillus acidophilus*. Biochim Biophys Acta - Gen Subj 1862:197–210. https://doi.org/10.1016/j.bbagen.2017.10.008

Wang X, Wang X, Wang T (2012) Synthesis of oleoylethanolamide using lipase. Agric Food Chem 60:451–457

Winkler UK, Stuckmann M (1979) Glycogen, hyaluronate and some other polysaccharides greatly enhance the formation of exolipase by *Serratia marcescens*. J Bacteriol 138:663–670

Xie C, Wu B, Qin S (2016) A lipase with broad solvent stability from *Burkholderia cepacia* RQ3: isolation, characteristics and application for chiral resolution of 1-phenylethanol. Bioprocess Biosyst Eng 39:59–66. https://doi.org/10.1007/s00449-015-1489-1

Yakun F, Yanjie Z, Yu X, Yi S, Zitao G, Youran L, Zhenghua G, Zhongyang D, Guiyang S, Liang Z (2021) Preparation and characterization of a novel thermostable lipase from *Thermomicrobium roseum*. Catal Sci Technol 11:7386–7397. https://doi.org/10.1039/D1CY01486B

Yasar G, Gulhan UG, Guduk E, Aktas F (2020) Screening, partial purification and characterization of the hyper-thermophilic lipase produced by a new isolate of *Bacillus subtilis* LP2. Biocatal Biotransform 38:367–375. https://doi.org/10.1080/10242422.2020.1751829

Zhao J, Ma M, Yan X, Zhang G, Xia J, Zeng G, Tian W, Bao X, Zeng Z, Yu P, Gong D (2022) Expression and characterization of a novel lipase from *Bacillus licheniformis* NCU CS-5 for application in enhancing fatty acids flavor release for low-fat cheeses. Food Chem 368:0308–8146. https://doi.org/10.1016/j.foodchem.2021.130868

Zhao J, Ma M, Zeng Z, Yu P, Gong D, Deng S (2021) Production, purification and biochemical characterisation of a novel lipase from a newly identified lipolytic bacterium *Staphylococcus caprae* NCU S6. J Enzyme Inhib Med Chem 36:249–257